

## Sustainable CO<sub>2</sub> Adsorbent via Amine-Phosphate Coupling of Glycated Chitosan and Electrochemically Exfoliated Graphene

Sucharita Pal<sup>a</sup>, Edward PL Roberts<sup>a</sup>, Milana Trifkovic<sup>a\*</sup> and Giovanniantonio Natale<sup>a\*</sup>

### Supporting Information

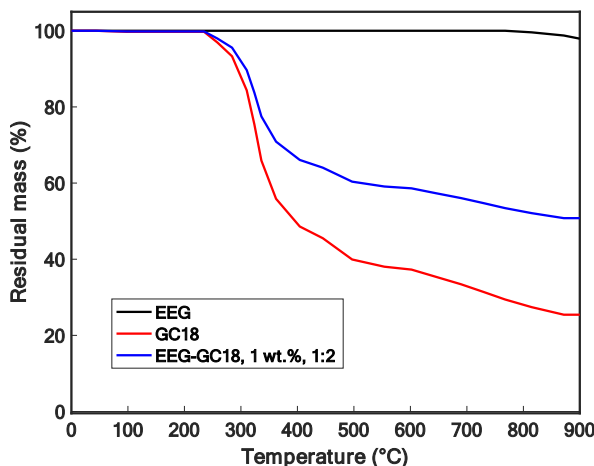


Figure S1. Thermogravimetric analysis of EEG, GC18 and EEG-GC18, 1 wt.%, 1:2 aerogel under N<sub>2</sub> gas.

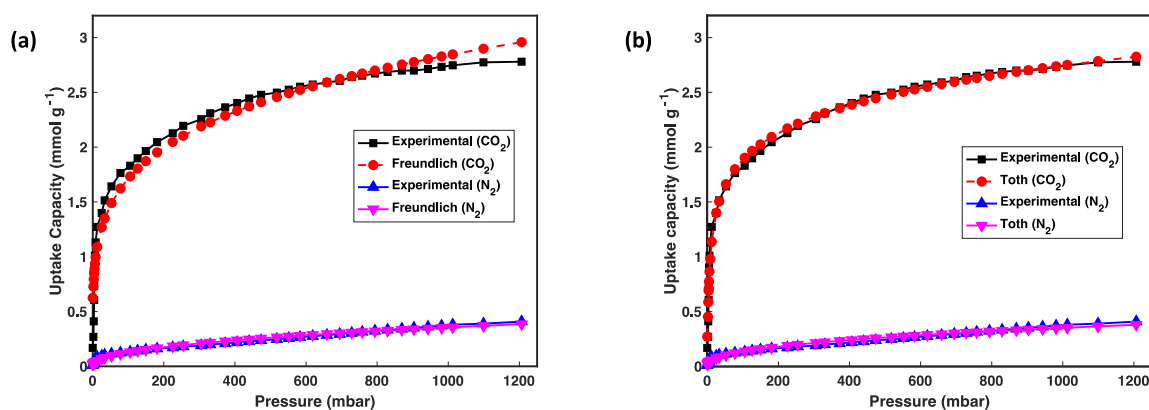


Figure S2. CO<sub>2</sub> and N<sub>2</sub> isotherms at 298 K on EEG-GC18 1 wt.%, 1:2 EEG: GC18 wt. ratio aerogels fitted to (a) Freundlich Model, (b) Toth Model.

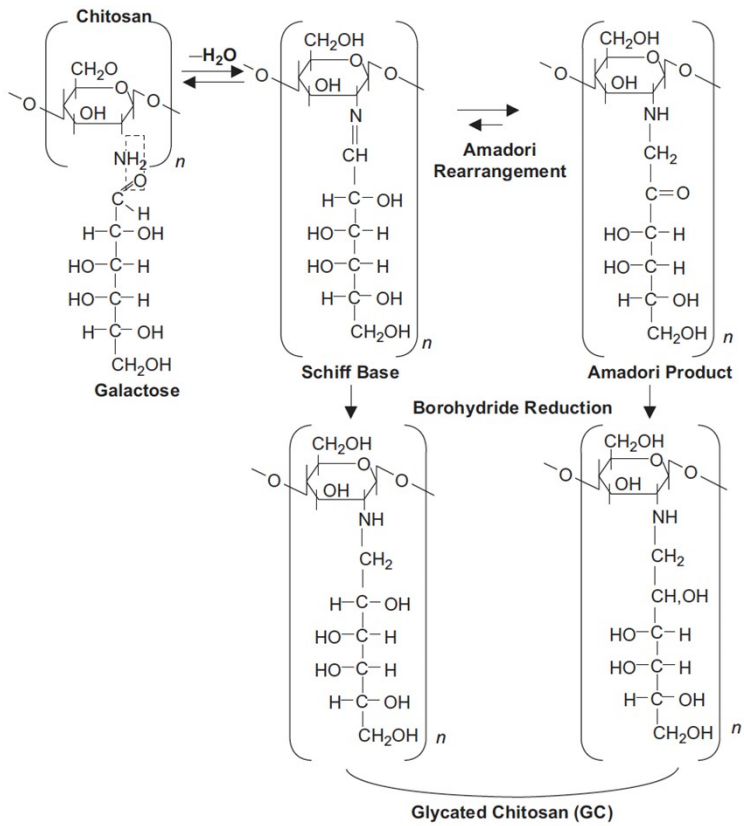


Figure S3. Reaction for the synthesis of glycated chitosan.

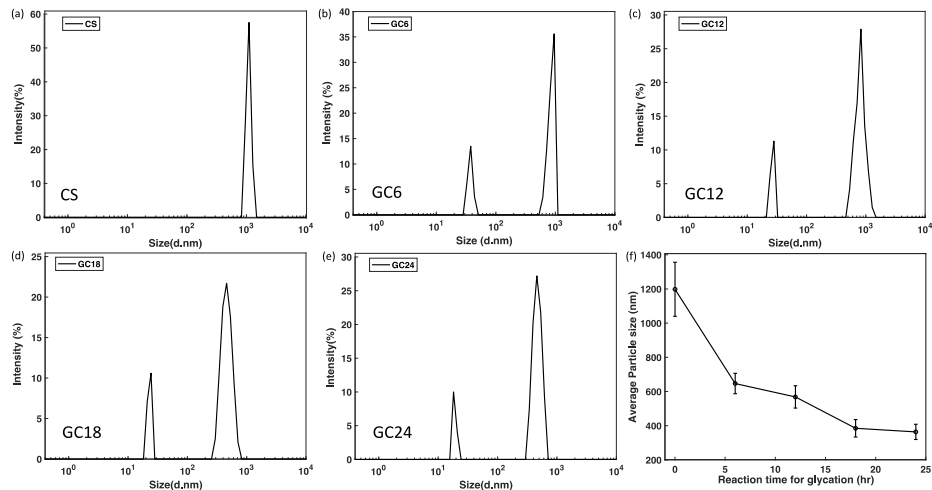


Figure S4. Particle size distribution of (a) CS (b) GC6 (c) GC12 (d) GC18 (e) GC24 (f) Average particle size of GC as a function of the extent of glycation in terms of reaction time, obtained from the Dynamic light scattering (DLS) method.

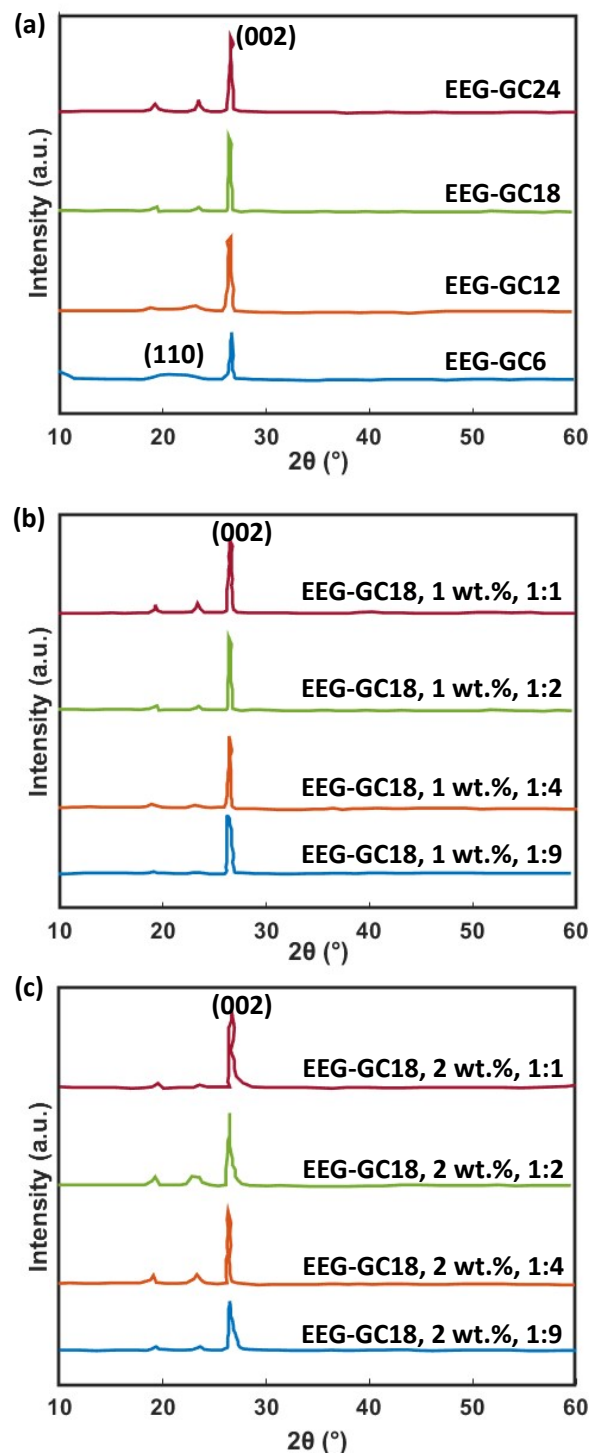


Figure S5. XRD patterns of (a) EEG-GC 1 wt.%, 1:2 EEG: GC wt. ratio aerogels, with varying extent of glycation, (b) 1 wt.% EEG: GC18 aerogels with varying EEG: GC wt. ratio, (c) 2 wt.% EEG: GC18 aerogels with varying EEG: GC wt. ratio.

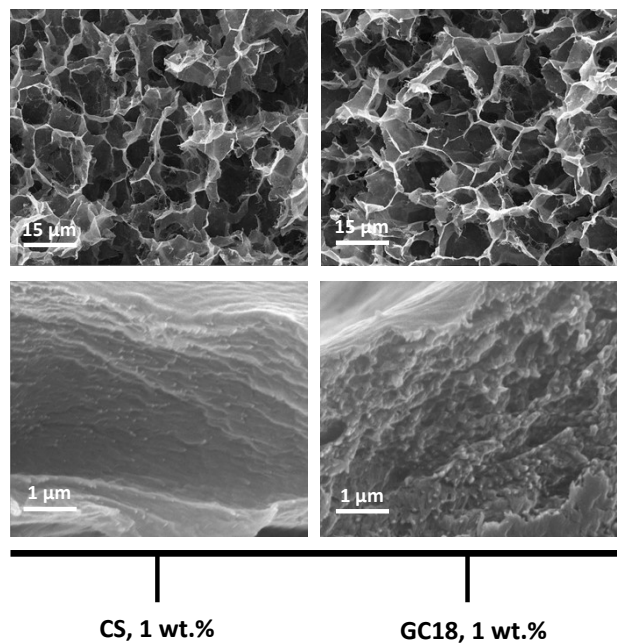


Figure S6. SEM images of 1 wt.% aerogels from CS and GC18, respectively. The top row for each case has a scale bar of 15  $\mu\text{m}$  while the bottom row has a scale bar of 1  $\mu\text{m}$ .

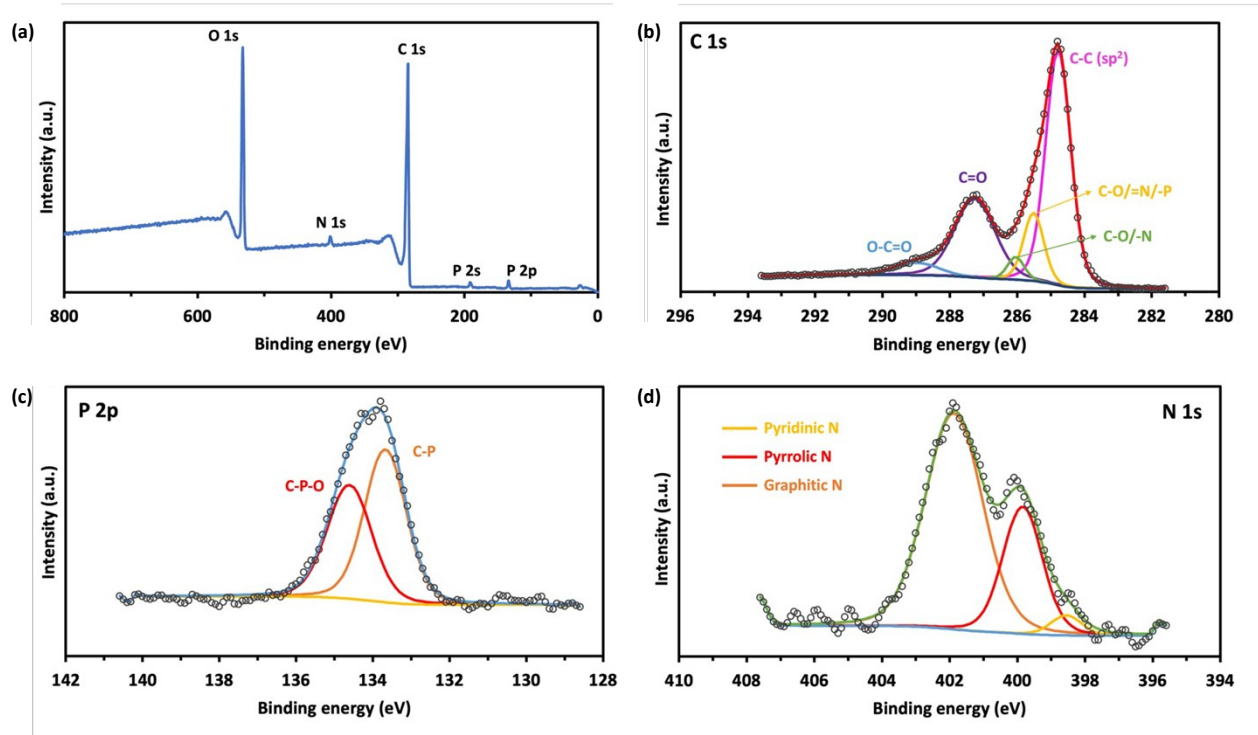


Figure S7. (a) Full-range XPS spectrum of EEG. High-resolution spectra of (b) C 1s (c) P 2p (d) N 1s.

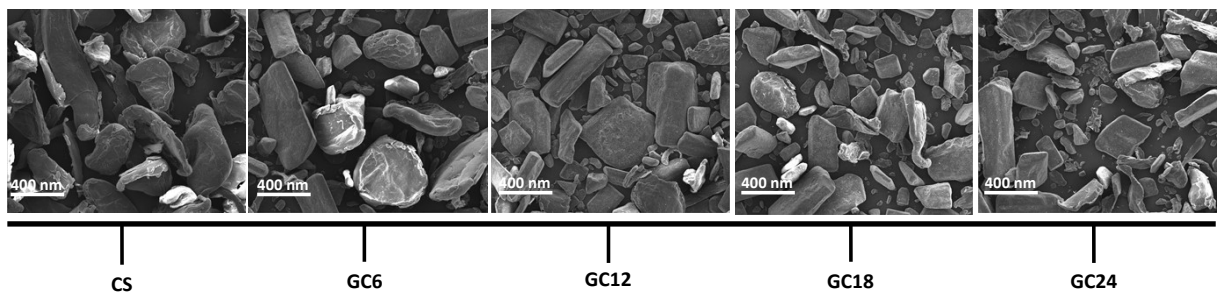


Figure S8. SEM images of pristine CS, and the synthesized GC6, GC12, GC18 and GC24 polymer particles. Each image has a scale bar of 400 nm.

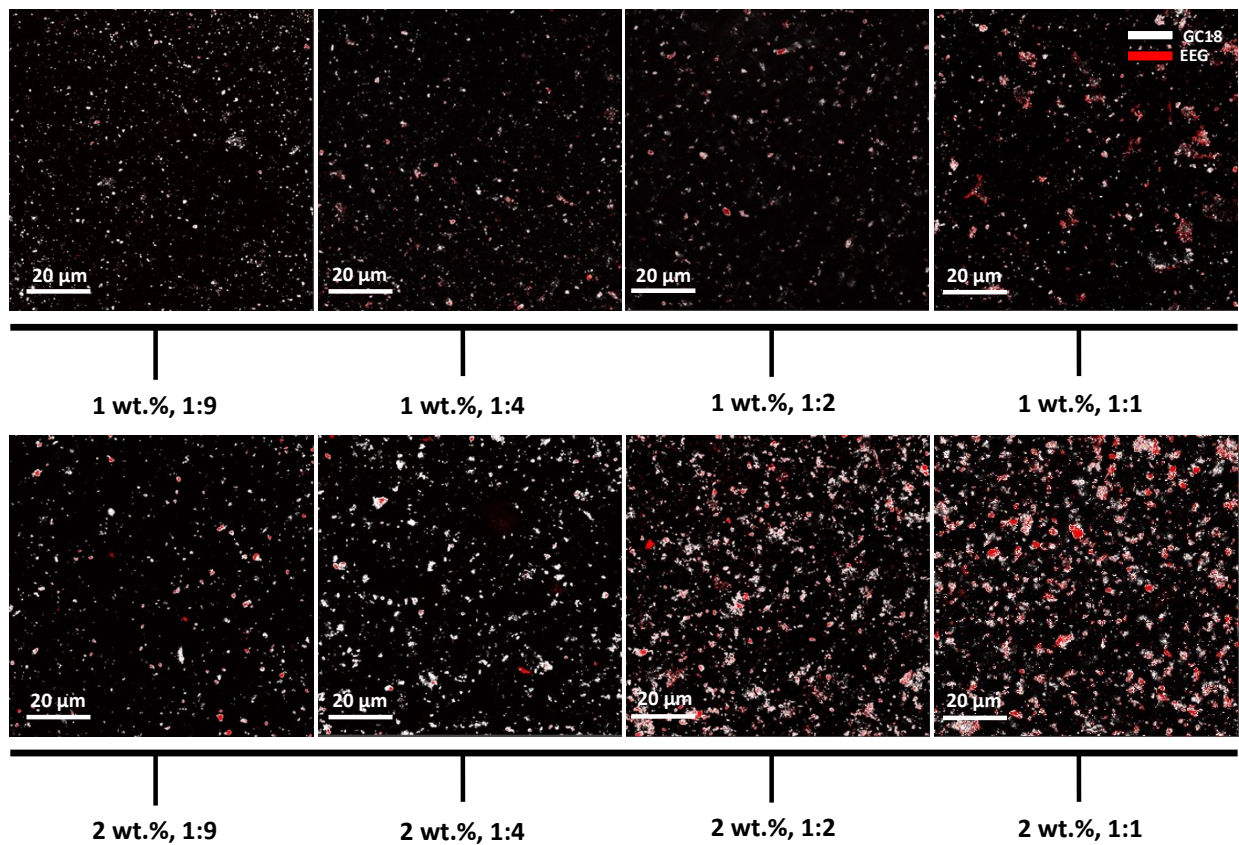


Figure S9. LSCM images of 1 wt.% and 2 wt.% EEG-GC18 precursor gels as a function of EEG: GC18 wt. ratio. and total solids content.

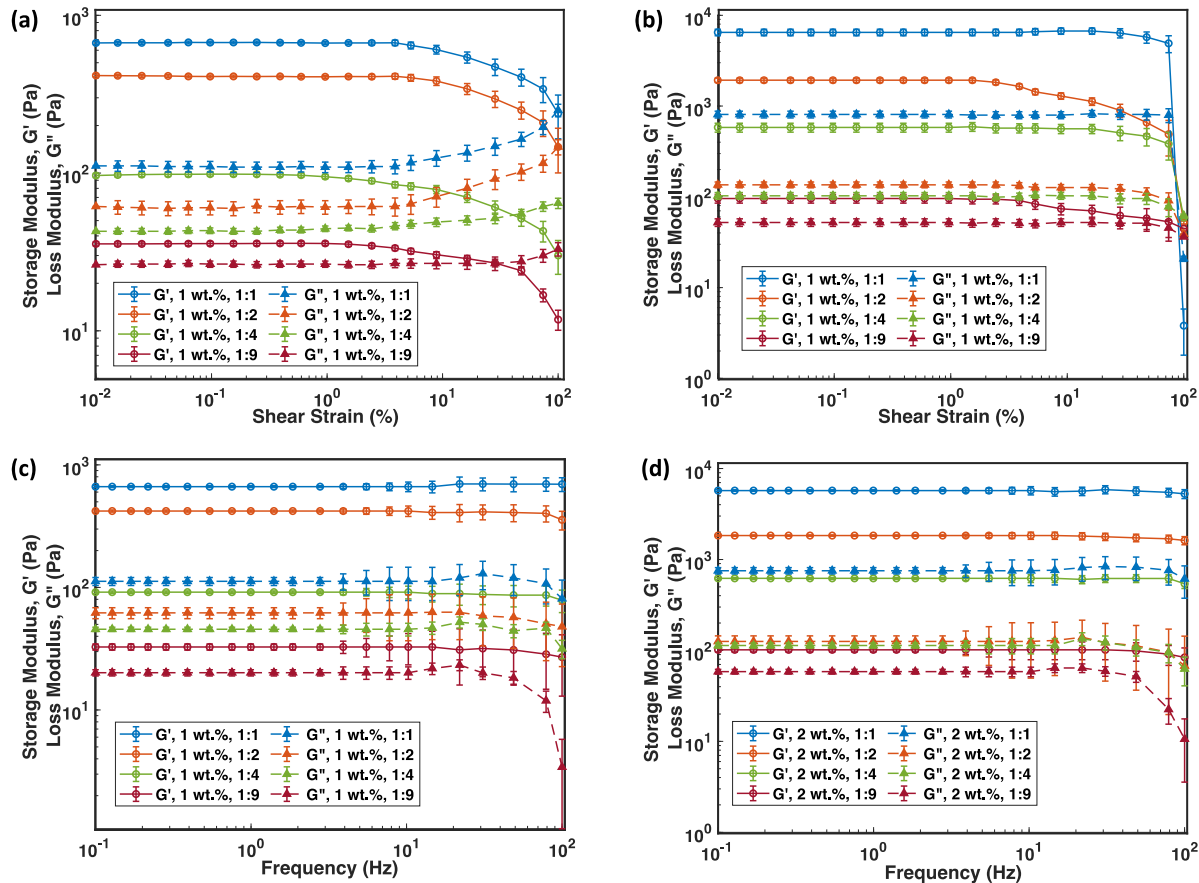


Figure S10. Rheological characterizations (Amplitude sweep) of EEG-GC18 mixed gels at different EEG: GC18 wt. ratios; percentage shows the amount of total solids content in the precursor gels, performed at a Frequency of 10 Hz (a) 1 wt.% EEG-GC18 and (b) 2 wt.% EEG-GC18. Rheological characterizations (Frequency sweep) of EEG-GC18 mixed gels at different EEG: GC18 wt. ratios; percentage shows the amount of total solids content in the precursor gels, performed at a Shear Strain of 1%. (c) 1 wt.% EEG-GC18 and (d) 2 wt.% EEG-GC18.

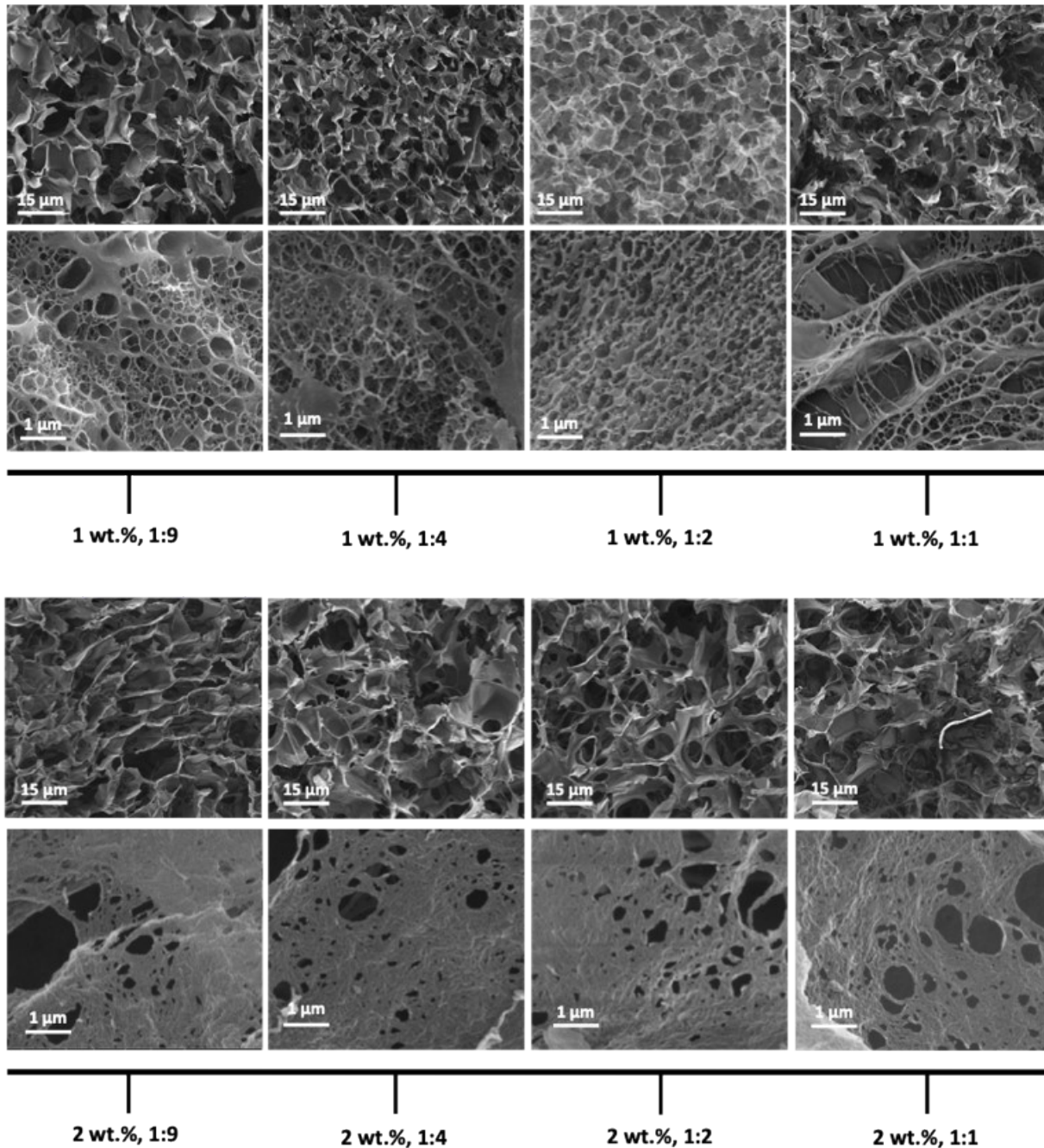


Figure S11. SEM images of 1 wt.% and 2 wt.% EEG: GC18 aerogels as a function of EEG: GC18 wt. ratio. The top row for each of the cases of 1 wt.% and 2 wt.% aerogels have a scale bar of 15 μm while the bottom row has a scale bar of 1 μm.

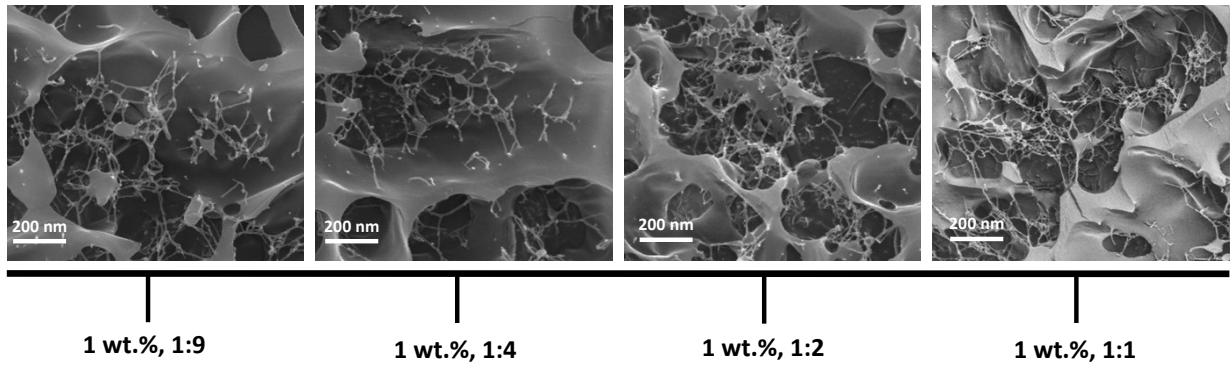


Figure S12. High magnification SEM images of 1 wt.% EEG: GC18 aerogels as a function of EEG: GC18 wt. ratio. Each image has a scale bar of 200 nm.

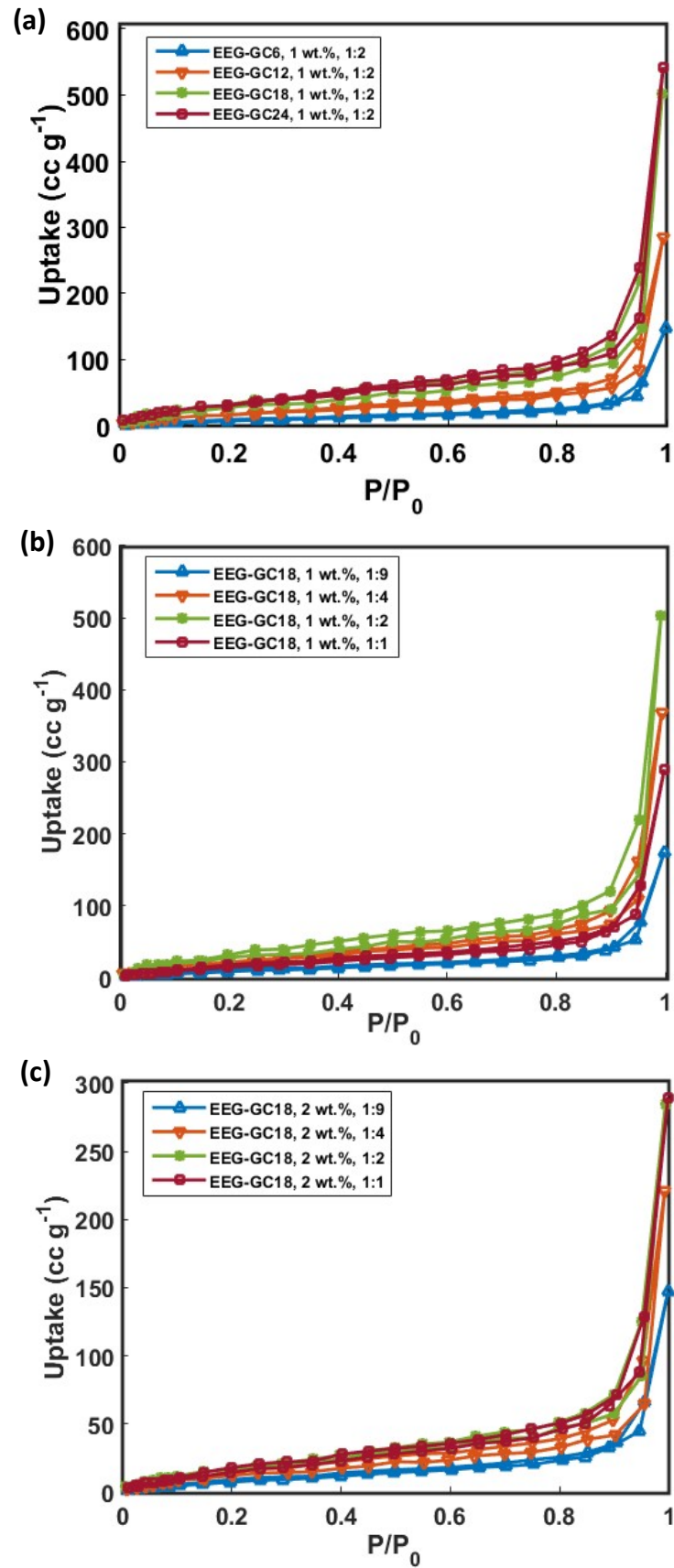


Figure S13. N<sub>2</sub> adsorption-desorption isotherm at 77 K of (a) EEG-GC 1 wt.%, 1:2 EEG: GC wt. ratio aerogels, with varying extent of glycation, (b) 1 wt.% EEG: GC18 aerogels with varying EEG: GC wt. ratio, (c) 2 wt.% EEG: GC18 aerogels with varying EEG: GC wt. ratio.

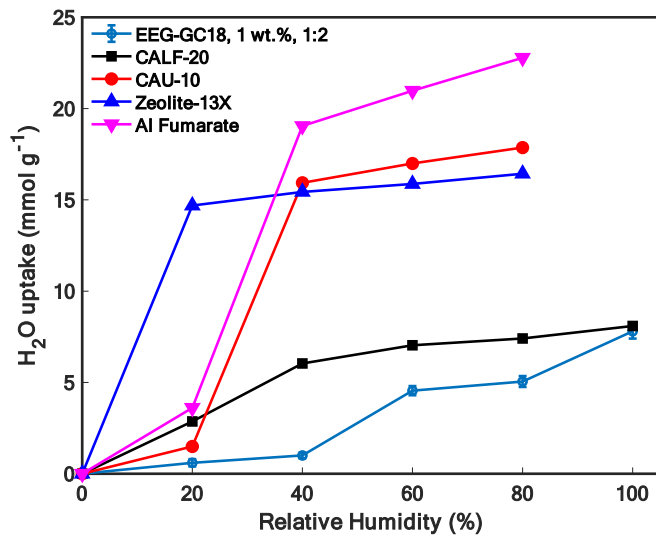


Figure S14. Comparison of H<sub>2</sub>O isotherm of different adsorbents at 298 K and 1 bar with EEG-GC18 1 wt.%, 1:2 EEG: GC18 wt. ratio aerogels as a function of relative humidity (%).<sup>[95-98]</sup>

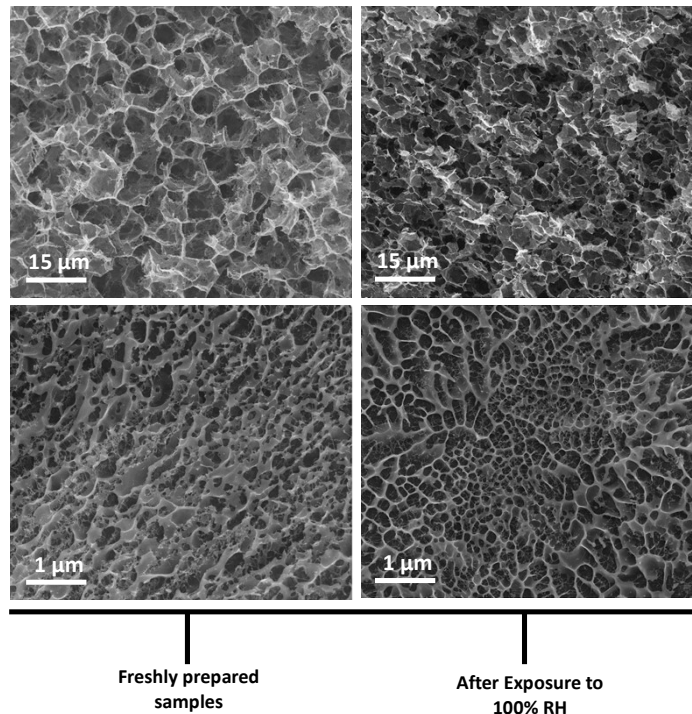


Figure S15. SEM images of EEG-GC18 1 wt.%, 1:2 aerogels before and after exposure to 100% RH. The top row for each case has a scale bar of 15 μm while the bottom row has a scale bar of 1 μm.

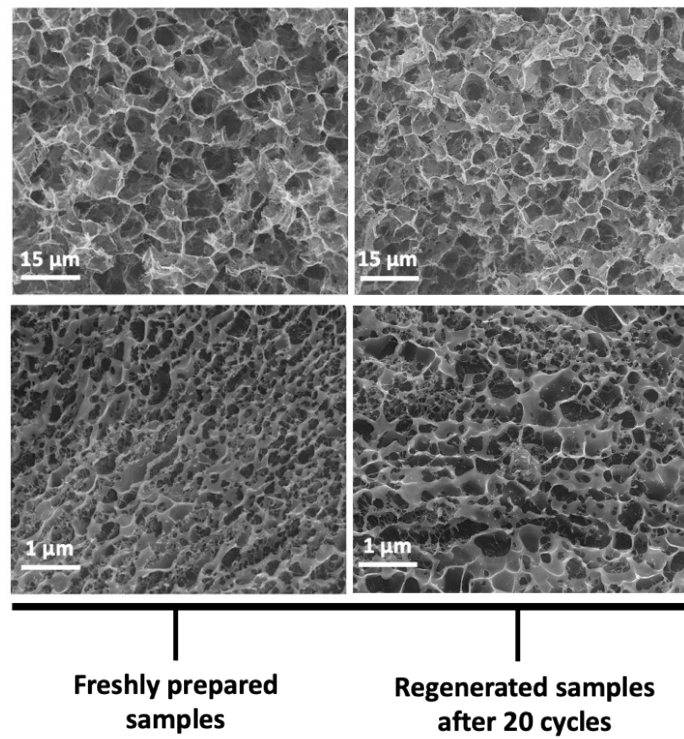


Figure S16. SEM images of the EEG-GC18 1 wt.%, 1:2 EEG: GC wt. ratio aerogels took before and after 20 adsorption- regeneration via. electrical heating. The top row for each of the cases has a scale bar of 15  $\mu\text{m}$  while the bottom row has a scale bar of 1  $\mu\text{m}$ .

Table S1. Characteristic results for different compositions of EEG-GC aerogels

Sample Composition	Bulk Density, $\rho_b$ ( $\text{g cm}^{-3}$ )	Porosity (%)	BET surface area ( $\text{m}^2\text{g}^{-1}$ )	Pore volume, $V_p$ ( $\text{cm}^3\text{g}^{-1}$ )	Average Diameter, $D_p$ (nm)	Pore CO <sub>2</sub> Uptake (mmol g <sup>-1</sup> ) (298 K; 1 bar)
EEG-GC18, 1 wt.% 1:9	0.058	94.5	91.6	0.27	7.50	2.56 ± 0.022
EEG-GC18, 1 wt.% 1:4	0.046	95.9	113.2	0.34	6.26	2.77 ± 0.026
EEG-GC6, 1 wt.% 1:2	0.093	85.1	53.6	0.16	12.89	1.68 ± 0.015
EEG-GC12, 1 wt.% 1:2	0.064	92.9	92.1	0.28	7.42	2.53 ± 0.03
EEG-GC18, 1 wt.% 1:2	0.039	97.8	136.3	0.41	5.11	2.88 ± 0.027
EEG-GC24, 1 wt.% 1:2	0.026	98.3	142.9	0.43	4.81	2.41 ± 0.02
EEG-GC18, 1 wt.% 1:1	0.027	97.2	127.6	0.38	5.47	2.66 ± 0.028
EEG-GC18, 2 wt.% 1:9	0.072	93.2	73.8	0.22	9.64	1.21 ± 0.028

EEG-GC18, 2 wt.% 1:4	0.065	94.2	82.4	0.25	8.49	$1.32 \pm 0.03$
EEG-GC18, 2 wt.% 1:2	0.048	96.1	90.5	0.27	9.17	$1.58 \pm 0.032$
EEG-GC18, 2 wt.% 1:1	0.051	96.3	78.2	0.23	10.70	$1.14 \pm 0.033$

Table S2. BET characterization results for SMP-GC18 and CSP-GC18 aerogels

Sample Composition	Bulk Density, $\rho_b$ (g cm <sup>-3</sup> )	Porosity (%)	BET surface area (m <sup>2</sup> g <sup>-1</sup> )	Pore volume, $V_p$ (cm <sup>3</sup> g <sup>-1</sup> )	Average Diameter, $D_p$ (nm)	Pore
SMP-GC18,	0.047	96.8	112.3	0.31	6.45	
1 wt.% 1:2						
CSP-GC18,	0.051	95.7	98.5	0.29	7.23	
1 wt.% 1:2						

Table S3. Fitting results for Freundlich and Toth models for CO<sub>2</sub> and N<sub>2</sub> adsorption data for EEG-GC18 1 wt.%, 1:2 aerogel at 298 K

Models	Correlation coefficients for CO <sub>2</sub> at 298 K			Correlation coefficients for N <sub>2</sub> at 298 K			$R^2$
	$k_F$	0.62	0.985	$k_F$	0.016	0.991	
Freundlich	$n$	4.56		$n$	2.26		
Toth	$q_s$	0.99	0.996	$q_s$	0.01	0.989	
	$k_T$	3.05		$k_T$	0.48		
	$m$	0.92		$m$	0.76		

Table S4. Comparison study of CO<sub>2</sub> adsorbents regenerated using electrical heating (Adsorption conditions: Pure CO<sub>2</sub>, 298 K and 1 bar)

Adsorbents	BET surface area (m <sup>2</sup> g <sup>-1</sup> )	CO <sub>2</sub> /N <sub>2</sub> Selectivity	CO <sub>2</sub> Uptake (mmol g <sup>-1</sup> )	Conductivity (S m <sup>-1</sup> )	Cycles studied; Regeneration efficiency	References
CNT-zeolite	—	33.6	4.2	58.6	3 cycles; 99%	[73]
MgAl-MMO/rGO aerogels	96.8	—	0.64	15	3 cycles; 99.5%	[74]
Activated carbon-Zeolite 13X	—	29.7	2.3	12.19	4 cycles: 98%	[75]
3D printed Zeolite 1985 13X/AC	1985	30.7	3.1	23.5	4 cycles; 90.4%	[76]
CNT films	562	—	3.96	48.1	8 cycles; 93.8%	[110]
PANI aerogels	94.2	—	2.14	28	5 cycles; 96%	[111]
EEG-GC18 aerogels	136.3	43.8	2.88	20.3 ± 0.2	20 cycles; 97%	This work

Table S5. Characteristic results for different compositions of EEG-GC aerogels, in terms of isosteric heatof adsorption.

Sample Composition	Isosteric heat of adsorption (kJ mol <sup>-1</sup> )
EEG-GC18, 1 wt.% 1:9	-47.6
EEG-GC18, 1 wt.% 1:4	-56.5
EEG-GC6, 1 wt.% 1:2	-43.4
EEG-GC12, 1 wt.% 1:2	-46.8
EEG-GC18, 1 wt.% 1:2	-57.8
EEG-GC24, 1 wt.% 1:2	-56.4
EEG-GC18, 1 wt.% 1:1	-39.4
EEG-GC18, 2 wt.% 1:9	-36.5
EEG-GC18, 2 wt.% 1:4	-37.9
EEG-GC18, 2 wt.% 1:2	-39.2
EEG-GC18, 2 wt.% 1:1	-35.8